Evaluation of Turbulence Induced Noise in Coherent Anti-Stokes Raman Scattering

by

Richard A. Elliott

Oregon Graduate Center

19600 N.W. Walker Road

Beaverton, Oregon 97006

NASA-Ames Grant No. NSG-2387

Final Technical Report

June 1, 1979 to December 31, 1982

The NASA Technical Officer for this Grant is

Dr. Robert L. McKenzie

NASA-Ames Research Center

Moffett Field, California 94035

Evaluation of Turbulence Induced Noise in Coherent Anti-Stokes Raman Scattering*

ABSTRACT

The effect of turbulence in a transonic wind tunnel on coherent anti-Stokes Raman scattering is considered. The driving pump and Stokes waves are taken to be coaxially propagating Gaussian beam waves which are focused on the Raman active medium through the turbulent boundary layer of the flow tube. The random index of refraction variations in the layer are modelled as phase perturbations of the driving waves which cause a reduction of the mean on-axis field and an increase in the mean diameter of the beams. Effective Gaussian beam parameters are developed and the radiated anti-Stokes power calculated as a function of the phase screen parameters. It is found that a significant reduction in signal strength occurs for realistic estimates of the phase screen parameter appropriate to a confined transonic flow. A method for estimating the signal degradation which could be applied to other experimental situations is presented.

*This work has been submitted for publication to the Journal of the Optical Society of America under the title "CARS Through a Turbulent Boundary."

I. Introduction

This project was concerned with the effects of turbulence on the coherent anti-Stokes Raman scattering (CARS) process as it might be used to monitor conditions in a transonic wind tunnel. CARS has already proven to be a valuable tool for remote, non-intrusive, sensing of molecular species concentration and temperature in flames,[1,2] combustion chambers[3] and high speed flows.[4,5] The major reasons for the great interest in CARS as a system probe stem from the facts that it does not perturb the system; it is capable of providing both spatial and temporal resolution; the signal is coherent and unidirectional thus providing excellent discrimination against background radiation; and both temperature and number density information can be extracted from it simultaneously.

It has been recently suggested that because of these properties CARS might be used to monitor conditions in transonic wind tunnels near test air foils. Since the gas flow under such circumstances is often turbulent, the effect of the random index of refraction variations due to turbulence on the CARS process is a matter of some importance. Since the flow in wind tunnels is most turbulent near the walls of the flow tube the situation can be modelled as a thin turbulent layer surrounding a quiescent laminar flow region.

CARS may be described in semi-classical macroscopic terms as a degenerate four wave mixing process mediated by a nonlinear susceptibility.[6] Two waves, a pump wave at frequency ω_1 and a

Stokes wave at frequency ω_2 shifted from the pump by the frequency of a Raman transition ($\omega_1 - \omega_2 = \nu$) drive the system and induce a polarization at $\omega_3 = \omega_1 + \nu$, the anti-Stokes frequency. This polarization field results in an emitted radiation field with each volume element in the interaction region producing a field at frequency ω_3 with a particular phase. For certain propagation directions, namely those for which the wave vectors satisfy the equation $2\vec{k}_1 - \vec{k}_2 - \vec{k}_3 = 0$, these radiated fields add in phase to produce a coherent anti-Stokes signal. In gaseous systems, with inconsequential dispersion, the three waves may be colinear and still satisfy the phase matching condition although other arrangements such as BOXCARS[7] are preferred in circumstances where spatial separation of the signal and driving waves is desired.

The theory of CARS generation in a homogeneous medium when the driving waves are coaxial Gaussian beam waves has been developed by Bjorklund.[8] His work takes into account explicitly the effects of dispersion and focusing of the driving beams. More recently Guha and Falk[9] have considered the problem from the point of view of optimal focusing and phase matching. The power of the anti-Stokes signal depends on the power of the Stokes beam and the square of the pump beam power. It increases asymptotically as the beams are more tightly focused and thus some loss of signal power is expected if for any reason the quality of the driving beams is degraded.

A medium with a time varying index of refraction causes a propagating laser beam to be deflected in a random manner and its instantaneous diameter to be broadened. If the refractive index variations are severe enough the irradiance pattern can even be broken into several independent patches. A turbulent layer could thus be expected to have a profound effect on CARS.

The problem of optical propagation in random media such as the turbulent atmospheric boundary layer has been thoroughly researched over the past two decades. One of the more fruitful formulations of the problem is the extended Huygens-Fresnel theory[10,11] which allows one to describe the statistical moments of the optical field in terms of the spatial spectrum of the index of refraction fluctuations.

The approach taken in the present work is to apply the Huygens-Fresnel formulation to CARS generation by coaxial Gaussian beams. First a brief review of the CARS process is presented and an explicit expression for the radiated anti-Stokes power developed. The effect of a turbulent layer on a propagating optical beam is then described and an expression for the anti-Stokes power derived when the pump and Stokes beams are perturbed by such a layer. Finally the loss in the CARS signal due to realistic estimates of the turbulence parameters in a transonic wind tunnel is determined.

II. CARS with Coaxial Gaussian Beam Waves

The development of the macroscopic theory of CARS presented here follows that published by Bjorklund.[8] The driving pump and Stokes waves at frequencies ω_1, ω_2 are assumed to be lowest order Gaussian modes propagating coaxially along the z axis with identical confocal parameters and beam waist locations. The beams are assumed to be linearly polarized in the same direction so that they may be treated as scalars and the total field written as a simple sum

$$E(\vec{r},t) = \mathrm{Re}\left[E_1(\vec{r})\ \exp(-i\omega_1 t) + E_2(\vec{r})\ \exp(-i\omega_2 t)\right] .$$

In the cylindrical coordinate system, transverse coordinate $\vec{\rho}$, axial coordinate z, the pump and Stokes field amplitudes take the form

$$\begin{aligned} E_j(\vec{r}) &\equiv E_j(\vec{\rho},z) \\ &= (k_j I_j/\pi b)^{1/2}\ (1 + 2iz/b)^{-1}\ \exp\left[ik_j z - k_j\rho^2/(b + 2iz)\right] \end{aligned} \tag{1}$$

with the confocal parameter $b = k_j w_{oj}^2$, w_{oj} being the beam radius at the waist ($z = 0$). The factor $(k_j I_j/b)^{1/2}$ normalizes the field so that the energy transmitted across any transverse plane

$$2\pi \int_0^\infty d\rho\rho\ E_j(\vec{\rho},z)\ E_j^*(\vec{\rho},z) = I_j,$$

a constant, independent of how tightly the beams are focused.

The effect of the pump and Stokes fields in the nonlinear medium is to produce a polarization wave at a frequency $\omega_3 = 2\omega_1 - \omega_2$, i.e.,

$$P(\vec{r},t) = \mathrm{Re}\left[P(\vec{r})e^{-i\omega_3 t}\right] \text{ with}$$

$$P(\vec{r}) = 3/4\ N\ \chi(-\omega_3;\ 2\omega_1,\ -\omega_2)\ E_1^2(\vec{r})\ E_2^*(\vec{r}) \tag{2}$$

where N is the number density of active atoms and χ is the nonlinear susceptibility per atom. The radiation field $E_3(\vec{r})$ generated from this polarization wave may be obtained by decomposing $P(\vec{r})$ into plane wave components with amplitude

$$P(\vec{K}) = (2\pi)^{-3} \int d^3r\ P(\vec{r})\ \exp(-i\vec{K}\cdot\vec{r}). \tag{3}$$

Each polarization plane wave component generates a radiating plane wave[12]

$$E_3(\vec{K};\vec{r}_o) = (2\pi k_o^2/k_3)\ \{1 - \exp[-i(z_o + L)\ (K_z - k_3 + \kappa^2/2k_3)]\}$$

$$\times\ (K_z - k_3 + \kappa^2/2k_3)^{-1}\ P(\vec{K})\ \exp(i\ \vec{K}\cdot\vec{r}_o) \tag{4}$$

with k_o being the vacuum wave vector and $\vec{K} \equiv (\vec{\kappa},K_z)$.

The total generated radiation field is the sum of these components

$$E_3(\vec{r}_o) = \int d^3K\ E(\vec{K};\vec{r}_o). \tag{5}$$

Using Eqs.(2), (3) and (4) in Eq.(5) and noting that the factor

$$\{1 - \exp[-i(z_o + L)(K_z - k_3 + \kappa^2/2k_3)\}(K_z - k_3 + \kappa^2/2k_3)^{-1}$$

can be written:

$$\int_{-L}^{z_o} \exp\{i[K_z - k_3 + \kappa^2/2k_3](z' - z_o)dz'$$

the result is

$$E_3(\vec{r}_o) = i\ 3/4\ N\chi(2\pi)^{-2}(k_o^2/k_3)\int d^3K \int_{-L}^{z_o} dz' \int d^3r \exp[i\vec{k}\cdot(\vec{r}_o - \vec{r})]$$

$$\times E_1^2(\vec{r})\ E_2^*(\vec{r})\ \exp\{i[K_z - k_3 + \kappa^2/2k_3](z' - z_o)\} \qquad (6)$$

In this form the integral over K_z may be performed immediately to give a factor $\delta(z' - z)$. The z' integration then gives

$$E_3(\vec{r}_o) \equiv E_3(\vec{\rho}_o, z_o)$$

$$= i(3N\chi k_o^2)/(16\ \pi^3 k_3) \int_{-L}^{z_o} dz \int d^2\rho\ E_1^2(\vec{r})E_2^*(\vec{r})$$

$$\times \int d^2\kappa \exp\{-ik_3(z - z_o) + i(z - z_o)\kappa^2/2k_3 + i\kappa\cdot(\vec{\rho}_o - \vec{\rho})\} \qquad (7)$$

In gaseous systems such as flames or wind tunnels dispersion is so slight that coaxial beams may have essentially perfect wavevector matching so that $\vec{k}_3 = 2\vec{k}_1 - \vec{k}_2$. When $E_1(\vec{r})$ and $E_2(\vec{r})$ as given by Eq.(1) are substituted into Eq.(7) then the integrals over κ and ρ may be evaluated to give

$$E_3(\vec{r}_o) = i(3N\chi k_o^2)(4k_3)^{-1}\,(k_1 I_1 I_2^{1/2} k_2^{1/2})(\pi b)^{-3/2}\exp(ik_3 z_o)$$

$$\times \int_{-L}^{z_o} dz\,(1 + 2iz/b)^{-1}\,[2k_1 + k_2 - 2ik_3 z/b]^{-1}\,[H(z_o,z)]^{-1}$$

$$\times \exp[-\rho_o^2/bH(z_o,z)] \qquad (8)$$

where

$$H(z_o,z) = \frac{1 + 4z^2/b^2}{2k_1 + k_2 - 2ik_3 z/b} - 2i\frac{(z - z_o)}{bk_3} \qquad (9)$$

Equation (8) gives the radiated anti-Stokes field for any $\vec{r}_o$. The quantity observed in experiments is of course the irradiance and the quantity of interest is the total power crossing the exit plane, $z = L_e$, of the system, i.e.

$$I_3(L_e) = 2\pi \int_o^\infty d\rho_o \rho_o\, E_3(\vec{\rho}_o,\, z_o = L_e)\, E_3^*(\vec{\rho}_o,\, z_o = L_e) \qquad (10)$$

Equation (10) along with (8) and (9) then provides the means to determine the strength of the anti-Stokes signal. The effect of tighter focusing, length of the interaction region, etc., may be examined and the configuration of the experiment optimized. For purposes of this report one important fact emerges: almost all the anti-Stokes signal is generated over a region within a distance of 5 times the confocal parameter of the beam waists,[13] $-5b < z < 5b$. This reduces the domain over which numerical integrations must be performed.

III. Optical Propagation Through a Turbulent Layer

The optical field at an observation point in a homogeneous medium due to a finite source can be expressed in terms of the Kirchoff integral which is the mathematical statement of the Huygens-Fresnel principle. The field amplitude at $\vec{r} \equiv (\vec{\rho},z)$, i.e., $E(\vec{\rho},z)$, due to a source distribution in the plane $\vec{s} \equiv (\vec{\sigma},z_1)$, i.e., $E(\vec{\sigma},z_1)$ with $z_1 < z$ is given by[14]

$$E(\vec{\rho},z) = (k/2\pi i)\cos\phi \int d^2\sigma \left|\vec{r}-\vec{s}\right|^{-1} \exp(ik\left|\vec{r}-\vec{s}\right|)\, E_o(\vec{\sigma},z_1) \quad (11)$$

where ϕ is the angle between $\vec{r}$ and the z axis. When the lateral dimensions of the source and the region of interest in the observation plane are much less than the distance from the source to the observation point the Fresnel approximations hold and

$$E(\vec{\rho},z) = [k/2\pi i(z-z_1)]\exp[ik(z-z_1)] \int d^2\sigma \exp[ik\left|\vec{\rho}-\vec{\sigma}\right|^2/2(z-z_1)] \times E_o(\vec{\sigma},z_1) \; . \quad (12)$$

The source distribution corresponding to a Gaussian beam wave in the plane $z = -L$ which converging to a focus at $z = 0$ is, from Eq.(1),

$$E_o(\vec{\sigma},-L) = (kI_o/\pi b)^{1/2}\,(1-2iL/b)^{-1} \exp[-ikL-k\sigma^2/(b-2iL)] \; . \quad (13)$$

If this expression for the source field is substituted into Eq.(12) and the integration performed Eq.(1) is recovered demonstrating the fact that the formulation is consistent.

The effect of a thin layer of turbulent gas on a laser beam propagating through it as illustrated in Figure 1 is to introduce random phase changes across the diameter of the beam which then

affect both the amplitude and phase of the field at locations remote from the turbulent layer. This situation may be modelled by introducing a random phase perturbation in the source field in Eq.(12) with statistical properties appropriate to the index of refraction fluctuations in the turbulent layer, i.e., the source field to be used in Eq.(12) is written as

$$E(\vec{\sigma},-L) = E_o(\vec{\sigma},-L) + \exp[i\psi(\vec{\sigma})] \tag{14}$$

where $E_o(\vec{\sigma},-L)$ is the unperturbed field and $\psi(\vec{\sigma})$ is the random phase function. The irradiance at a point $\vec{r}$ due to this source field is then from Eqs.(12), (13) and (14).

$$\begin{aligned} I(\vec{r}) &= E(\vec{\rho},z)\, E^*(\vec{\rho},z) \\ &= (k^3 I_o)\, [4\pi^3 b\, (z+L)^2\, (1 + 4L^2 b^2)]^{-1} \\ &\times \iint d^2\sigma_1\, d^2\sigma_2 \exp\{ik[|\vec{\rho}-\vec{\sigma}_1|^2 - |\vec{\rho}-\vec{\sigma}_2|^2]/2(z+L)\} \\ &\times \exp\{-k\sigma_1^2/(b-2iL) - k\sigma_2^2/(b+2iL) + i\psi(\vec{\sigma}_1) - i\psi(\sigma_2)\} \end{aligned} \tag{15}$$

and the mean irradiance

$$\begin{aligned} \langle I(\vec{r})\rangle &= k^3 I_o [4\pi^3 b(z+L)^2(1 + 4L^2/b^2)]^{-1} \\ &\times \iint d^2\sigma_1\, d^2\sigma_2 \exp\{-k\sigma_1^2/(b-2iL) - k\sigma_2^2/(b+2iL) \\ &+ ik[|\vec{\rho}-\vec{\sigma}_1|^2 - |\vec{\rho}-\vec{\sigma}_2|^2]/2(z+L)\} \\ &\times \langle \exp[i\psi(\vec{\sigma}_1) - i\psi(\vec{\sigma}_2)]\rangle \end{aligned} \tag{16}$$

This differs from the same quantity in the absence of the turbulent layer (phase screen) only by the last term, $\langle \exp[i\psi(\vec{\sigma}_1) - i\psi(\vec{\sigma}_2)] \rangle$, and its form is determined by the characteristics of the turbulent layer.

The index of refraction in a turbulent region can be described in statistical terms. It is usual to write it as $n(\vec{r}) = 1 + n_1(\vec{r})$ with $n_1(\vec{r})$ being a zero mean Gaussian random function and to assume that the turbulence is isotropic and statistically homogeneous. In this case the two point correlation function of the index of refraction fluctuations

$$B_n(\vec{r}_1,\vec{r}_2) \equiv \langle n_1(\vec{r}_1)\, n_1(\vec{r}_2) \rangle \tag{17}$$

depends only on the separation of the two points

$$B_n(\vec{r}_1-\vec{r}_2) = B_n(|\vec{r}_1-\vec{r}_2|) = B_n(r) \tag{18}$$

The spatial spectrum of the index of refraction fluctuations, the 3-D Fourier transform of $B_n(r)$, is commonly taken to be the modified Von Karman spectrum[10]

$$\phi_n(K) = C_n^2 (K^2 + K_o^2)^{-11/6} \exp(-K^2/K_m^2). \tag{19}$$

Here K_o and K_m are the wave numbers corresponding to the largest and smallest scale sizes of the turbulent eddies respectively and C_n^2 is a measure of the strength of turbulence related to the variance $\langle n_1^2 \rangle$ by the fact that

$$\langle n_1^2 \rangle = B_n(0) = \int d^3K\ \phi_n(K). \tag{20}$$

For, if $K_o \ll K_m$ performing the integration yields

$$\begin{aligned}\langle n_1^2 \rangle &= 2\pi\Gamma(3/2)\Gamma(1/3)[\Gamma(11/6)]^{-1}K_o^{-2/3}\ C_n^2 \\ &= 15.9\ K_o^{-2/3}\ C_n^2\end{aligned} \tag{21}$$

The random phase screen corresponding to a thin layer of turbulence of thickness Δz with the spectrum of Eq.(10) is then such that[15]

$$\begin{aligned}\langle \exp[i\psi(\vec{\sigma}_1) - i\psi(\vec{\sigma}_2)] \rangle &= \exp\{-2[\langle \psi^2 \rangle - B_\psi(\vec{\sigma}_1, \vec{\sigma}_2)]\} \\ &= \exp\{-4\pi^2 k^2 \Delta z \int dKK\ \phi_n(K)[1 - J_o(K\sigma_{12})]\} \\ &\equiv \exp\{-D_\psi(\sigma_{12})\}\end{aligned} \tag{22}$$

with $\sigma_{12} = |\vec{\sigma}_1 - \vec{\sigma}_2|$. $B_\psi(\vec{\sigma}_1, \vec{\sigma}_2)$ is the phase correlation function in the plane and $D_\psi(\sigma_{12})$ is called the phase structure function. The variance of the phase[16]

$$\begin{aligned}\langle \psi^2 \rangle &= 2\pi^2 k^2 \Delta z \int dKK\ \phi_n(K) \\ &= (12\pi^2/5)\ K_o^{-5/3}\ C_n^2\ k^2\ \Delta z \\ &= 23.69\ K_o^{-5/3}\ C_n^2\ k^2\ \Delta z.\end{aligned} \tag{23}$$

There are two regimes for which the expression for D_ψ simplifies. If $\sigma K_m \ll 1$, then the Bessel function may be expanded in series and the integral performed term by term to yield[16]

$$D_\psi(\sigma_{12}) = 27.48\ k^2\ C_n^2\ \Delta z\ (K_m^{1/3} - 1.09\ K_o^{1/3})\ \sigma_{12}^2 \qquad (24)$$

On the other hand if $\sigma K_m >> 1$ the exponential factor in $\phi_n(K)$ may be replaced by unity and the integral evaluated to give for the phase structure function[17,18]

$$\begin{aligned} D_\psi(\sigma_{12}) &= 44.06\ k^2\ C_n^2\ \Delta z\ \sigma_{12}^{5/3} \\ &= 1.86\ \langle\psi^2\rangle\ K_o^{5/3}\ \sigma_{12}^{5/3} \\ &\equiv A_\psi \sigma_{12}^{5/3} \end{aligned} \qquad (25)$$

These two regimes correspond to two quite different physical situations. The first corresponds to the case where phase correlations are of interest only over a span which is smaller than K_m^{-1}, i.e., the scale size of the smallest turbulent eddies. This would be the case if the diameter of the laser beam at the phase screen were smaller than K_m^{-1}. The quadratic behavior describes the situation in which the beam is deflected but the wavefront across the beam is not distorted and the beam is not otherwise affected.[19] The second regime corresponds to the case of a beam much larger in diameter than the smallest eddies and the $\sigma_{12}^{5/3}$ dependence indicates that the wavefronts across the beam are distorted leading to an increase in the diameter of the beam farther down the propagation path and a consequent loss of power density.

The effect that a phase screen or a thin turbulent layer has on CARS depends on several factors. For the case of coaxial focused Gaussian beams with the beam waists located some distance from the phase screen as illustrated in Figure 1 both the pump and Stokes waves experience identical phase changes. Hence there is no loss of coherence relative to each other, the wave vector matching condition is not affected and only the loss in power density in the focal region of the beams due to the turbulence affects the anti-Stokes power. If the beam diameter at the phase screen is smaller than the smallest turbulence scales the only effect will be a random steering of the beams without loss of power density and the anti-Stokes radiation will be unchanged except for a random variation in the propagation direction. On the other hand if the laser beams are not coaxial as is the case, for example, in BOXCARS, the random deflection of the pump and Stokes waves are not identical and may be completely uncorrelated depending on their separation and the largest turbulence scale size. In this case a considerable disruption of the coherence and overlap of the laser beams may occur and the resulting CARS signal be severely affected.

Since deflection of coaxial pump and Stokes beams without a change in the instantaneous beam waist diameters does not change the magnitude of the measured CARS signal there is no appreciable effect in the case where the beam diameters in the turbulent layer are smaller than the smallest turbulence scale, K_m^{-1}. In

practice this condition would obtain only in very large flow tubes. In most cases it is necessary then to consider the effect on the pump and Stokes power densities in the focal region generated by a phase screen whose correlations are described by Eq.(25).

Insertion of Eq.(25) into Eq.(16), making the change of variables, $\vec{\sigma} = \vec{\sigma}_1 - \vec{\sigma}_2$, $\vec{S} = \vec{\sigma}_1 + \vec{\sigma}_2$, and integrating over S gives

$$I(\vec{r}) = I_o k^2 [4\pi^2 (z + L)^2]^{-1} \int d^2\sigma \exp\{-ik\vec{\sigma}\cdot\vec{r}/(z + L) - k(4z^2 + b^2)\sigma^2/[8b(z + L)^2] - A_\psi \sigma^{5/3}\} \quad (26)$$

The angular part of the integration can be performed in turn to yield[20]

$$I(\vec{r}) = I_o k^2 [2\pi (z + L)^2]^{-1} \int_o^\infty d\sigma\, \sigma\, J_o[kr\sigma/(z + L)] \times \exp\{-k\sigma^2(4z^2 + b^2)/[8b(z + L)^2] - A_\psi \sigma^{5/3}\} \quad (27)$$

Since the CARS signal is produced mainly in the focal region, $z \approx 0$, and typically $kb\sigma^2/L^2 >> A_\psi \sigma^{5/3}$ the turbulence term may be regarded as small and $\exp\{-A_\psi \sigma^{5/3}\}$ expanded in series. The remaining integration in Eq.(26) may then be accomplished term by term.[21] Retaining only the first two terms one has

$$I(r) \approx \pi^{-1} I_o kb(4z^2 + b^2)^{-1} \{\exp[2kbr^2/(4z^2 + b^2)]$$

$$- A_\psi \Gamma(11/6)[k(4z^2 + b^2)/(8b(z + L)^2)]^{-5/6}$$

$$\times {}_1F_1(11/6;1; -2kbr^2/(4z^2 + b^2))\}$$

$$= \pi^{-1} I_o kb(4z^2 + b^2)^{-1} \exp[-2kbr^2/(4z^2 + b^2)]$$

$$\times \{1 - A_\psi \Gamma(11/6)[k(4z^2 + b^2)]^{-5/6} [8b(z + L)^2]^{5/6}$$

$$\times {}_1F_1(-5/6;1; 2kbr^2/(4z^2 + b^2))\} \qquad (28)$$

where ${}_1F_1(a;b;z)$ is the confluent hypergeometric function and Kummers transformation[22] has been used. The distribution $I(r)$ given in Eq.(28) is nearly gaussian and may be conveniently approximated by

$$I_1(r) = \pi^{-1} I_o kb^2 \beta^{-1}(z) (4z^2 + b^2)^{-1}$$

$$\times \exp\{-2kb^2 r^2 [\beta(z)(4z^2 + b^2)]^{-1}\} \qquad (29)$$

with

$$\beta(z) = b\{1 + (5/6) A_\psi \Gamma(11/6) (8b/k)^{5/6} (z + L)^{5/3} (b^2 + 4z^2)^{-5/6}\} \qquad (30)$$

The factor $\beta(z)$ represents additional beam spreading due to the phase screen. For example at the beam waist, $z = 0$, the beam radius is larger by a factor $[1 + (5/6) A_\psi \Gamma(11/6) (8/bk)^{5/6} L^{5/3}]$. The appropriate expression for the field in the presence of a phase screen at $z = -L$ instead of that given in Eq.(1) is then

$$\tilde{E}_j(\bar{r}) = (k_j I_j/\pi)^{1/2}\,[\beta(z)]^{-1/2}(1 + 2iz/b)^{-1}$$

$$\times \exp\{ik_j z - k_j\rho^2\, b[\beta(z)(b + 2iz)]^{-1}\} \qquad (31)$$

and this expression should be used to represent the fields of the pump and Stokes beams for calculation of the CARS intensity as given in Eq.(7). Although $\beta(z)$ does depend somewhat on the wavelength of the radiation through the $k^{-5/6}$ factor the difference between the pump and Stokes wavelengths is sufficiently small that one may use the pump wavevector, k_1, throughout with negligible error.

IV. Loss of CARS Intensity Due to a Turbulent Layer

The total radiated anti-Stokes power in the absence of turbulence may be calculated from Eqs.(8), (9), and (10). The effect of a turbulent layer in the path of the pump and Stokes driving waves remote from the focal region is to induce a reduction in the on-axis amplitude and an increase in the effective diameter of the driving beams. Substitution of the expression given in Eq.(31) for the pump and Stokes fields in Eq.(7) and evaluation of the integrals over κ and ρ yields an equation similar to Eq.(8):

$$\tilde{E}_3(\vec{r}_o) = i(3N\chi k_o^{\,2})\pi^{-3/2}\,(4k_3)^{-1}(k_1 I_1 k_2^{\,1/2} I_2^{\,1/2})\,\exp(ik_3 z_o)$$

$$\times \int_{-L}^{z_o} dz(1 + 2iz/b)^{-1}\,\beta^{-1/2}(z)\,[2k_1 + k_2 - 2ik_3 z/b]^{-1}$$

$$\times [H_T(z_o,z)]^{-1}\,\exp[-\rho_o^{\,2}/bH_T(z_o,z)] \qquad (32)$$

$$\text{with } H_T(z_o,z) = \frac{\beta(z)(1 + 4z^2/b^2)}{b(2k_1 + k_2 - 2ik_3z/b)} - 2i\,\frac{(z - z_o)}{bk_3} \tag{33}$$

The total anti-Stokes power radiated is then

$$\tilde{I}_3(L_e) = 2\pi \int_o^\infty d\rho_o \rho_o \left|\tilde{E}_3(\bar{\rho}_o; z_o = L_e)\right|^2 \tag{34}$$

which may be rewritten using Eq.(32) as a double integral

$$\tilde{I}_3(L_e) = 9N^2X^2k_o^4\,(4\pi k_3)^{-2}\,k_1^2I_1^2k_2I_2$$

$$\times \int_{-L}^{L_e}\int dz_1dz_2(1 + 2iz_1/b)^{-1}(1 - 2iz_2/b)^{-1}$$

$$\times \beta^{-1/2}(z_1)\,\beta^{-1/2}(z_2)\,[2k_1 + k_2 - 2ik_3z_1/b]^{-1}$$

$$\times [2k_1 + k_2 + 2ik_2/b]^{-1}\,[H_T(L_e,z_1) + H_T^*(L_e, z_2)]^{-1} \tag{35}$$

As stated earlier at the end of Section II the major contribution to the CARS signal arises within a distance equal to ten times the confocal parameter of the beam waist.[13] All lengths along the propagation path may be scaled in units of the confocal parameter, i.e., the dimensionless variables $x_{1,2} = 2z_{1,2}/b$ may be defined and the range of integrations restricted to $-10 < x_{1,2} < 10$ to give assuming $L > 5b$ and $L_e > 5b$,

$$\tilde{I}_3(\ell_e) = 9N^2X^2k_o^4(4\pi k_3)^{-2}\, k_1^2\, I_1^2\, k_2\, I_2\, b^{-1}$$

$$\times \int_{-10}^{10}\int dx_1dx_2\, (1 + ix_1)^{-1}(1 - ix_2)^{-1}\gamma^{-1/2}(x_1)\, \gamma^{-1/2}(x_2)$$

$$\times [2k_1 + k_2 - ik_3x_1]^{-1}[2k_1 + k_2 + ik_3x_2]^{-1}$$

$$\times [H_T(\ell_e,x_1) + H_T^*(\ell_e,x_2)]^{-1} \qquad (36)$$

where $\ell_e = 2L_e/b$, $\ell = 2L/b$,

$$\gamma(x) = \beta(x)/b = [1+(5/6)A_\psi\Gamma(11/6)(2b/k_1)^{-5/6}(x+\ell)^{5/3}(1+x)^{-5/6}]$$

and $$H_T(\ell_e,x) = \frac{\gamma(x)(1+x^2)}{2k_1+k_2-2ik_3x} - i\,\frac{x-\ell_e}{k_3} \qquad (37)$$

The integrals in Eq.(36) must be evaluated numerically. However, if $\ell \gg 10$, i.e. $L \gg 5b$, within the range of integration

$$\gamma(x) \approx \gamma(o) = 1 + (5/6)A_\psi\Gamma(11/6)(2b/k)^{5/6}\, \ell^{5/3}. \qquad (38)$$

Moreover the $\gamma^{-1/2}(x_1)\gamma^{-1/2}(x_2)$ factors are dominant compared to those involved in H_T and H_T^*. In this approximation the signal in the presence of a turbulent layer is just $\gamma^{-1}(o)$ times that in the absence of turbulence, i.e., the ratio

$$I_3/\tilde{I}_3 = \gamma(o)$$

$$= 1 + (5/6)A_\psi\Gamma(11/6)(2b/k_1)^{5/6}\, \ell^{5/3}$$

$$= 1 + (5/6)A_\psi\Gamma(11/6)(8/bk_1)^{5/6}\, L^{5/3}$$

$$= 1 + 4.43\, A_\psi(bk_1)^{-5/6}\, L^{5/3}. \qquad (39)$$

Thus, in this approximation, the ratio of the CARS signal in the absence of turbulence to that generated through a turbulent layer varies linearly with the strength of turbulence through the factor A_ψ; it varies as $b^{-5/6}$ so that tighter focusing, i.e., decreasing b, is detrimental; and the 5/3 power dependence on the distance from the turbulent layer to the focal region imposes a restraint on the region which may be explored through a turbulent layer. The validity of the approximation and the behavior expected for realistic estimates of the parameters involved is illustrated in Figures 2 and 3 where $\ell n(I_3/\tilde{I}_3)$ calculated from Eq.(39) and the value determined from numerical integration of Eq.(36) are plotted as functions of the distance between the phase screen and focal region, L. The pump, Stokes and anti-Stokes wavelengths are assumed to be 532 nm, 557 nm and 509 nm respectively for purposes of this illustration.

The values of A_ψ used to generate the data displayed in the figures were calculated on the basis of some assumptions of the characteristics of the turbulent boundary layer. Referring to Eq.(25), $A_\psi = 44.06\ k_1^2\ C_n^2\ \Delta z$, Δz being the thickness of the turbulent layer and C_n^2 being the strength of turbulence parameter which is related to the variance in index of refraction $\langle n_1^2 \rangle$ and the wave number of the largest scale turbulent eddies K_o through Eq.(21). For this illustration it is assumed that

the phase screen models the turbulent boundary layer in a mach 2.5 flow in a rectangular nozzle of 50 cm^2 cross-sectional area. Typical characteristics for this type of flow[23] are $\Delta z \approx 5$ mm, $K_o \approx 3.1\ cm^{-1}$, $K_m \approx 630\ cm^{-1}$ and the rms density fluctuations $\langle(\Delta\rho/\rho)^2\rangle^{1/2}$ may be as great as 5%. The index of refraction of air varies linearly with density with the deviation from unity, $n_1 = 3 \times 10^{-4}\ (\Delta\rho/\rho)$. Thus $\langle n_1^2\rangle \lesssim 2 \times 10^{-10}$, the strength of turbulence parameter $C_n^2 \lesssim 2 \times 10^{-11}\ cm^{-2/3}$, the phase variance $\langle\psi^2\rangle \lesssim 0.5$ and $A_\psi \lesssim 6\ cm^{-5/3}$. The values of A_ψ used in the following calculations are 0.6 and 6 $cm^{-5/3}$ corresponding to rms density fluctuations of 0.5% and 5%.

Two values of the confocal parameter were also chosen for purposes of illustration: b = 2.2 mm and 0.14 mm, corresponding to focusing a 1 cm diameter collimated beam with 40 and 10 cm focal length lenses respectively. Rewriting Eq.(39) as

$$I_3/\tilde{I}_3 = 1 + \alpha L^{5/3} \tag{40}$$

with $\alpha = 4.43\ A_\psi (bk_1)^{-5/6}$ the value b = 0.14 mm generates values of $\alpha = 5.5 \times 10^{-2}$ and $5.5 \times 10^{-3}\ cm^{-5/3}$ for $A_\psi = 0.6$ and 6 $cm^{-5/3}$ respectively. Curves of $\ell n(I_3/\tilde{I}_3)$ calculated from Eq.(40) with these values of α are plotted in Figure 2 along with the numerical integration results. Similar curves for b = 2.2 mm, $\alpha = 5.5 \times 10^{-4}$ and $5.5 \times 10^{-3}\ cm^{-5/3}$ are plotted in Figure 3. In both cases it is seen that a significant loss of signal can occur. For example, rms density fluctuations of 5% cause a factor

of 2 loss in signal if the turbulent layer is 5.7 cm from the focus of a 10 cm focal length lens (Figure 2).

V. Discussion

It is clear from Figures 2 and 3 that the approximation invoked in deducing Eq.(39) from Eq.(36) is reasonably accurate over a substantial range of separation of the phase screen and focal region, L, turbulence strength, A_ψ, and beam geometry, b. Based on the indicated functional dependence it may be concluded that it is advantageous to reduce as far as possible the separation of the focal region and the turbulent layer and to focus the beam less tightly, i.e., increase b. Of course it is in general not possible to choose the distance between the focus and the boundary layer. Nor is it always desirable to increase the confocal parameter since that implies an increase in the beam diameters and the length of the region in which the signal is generated with a concomitant loss in spatial resolution.

The results presented were calculated for turbulence strengths and scale sizes which are typical of transonic flows in small nozzles and the tightness of focus of the driving beams was chosen to conform to a typical laboratory experiment. Application of these results to CARS in flames, jets and other high speed flows should also be possible. In order to do so one would need values for the rms density fluctuations, $\langle(\Delta\rho/\rho)^2\rangle^{1/2}$, in the turbulent boundary between the flame or jet and the surrounding atmosphere as well as the thickness of the layer, Δz, and the largest turbulence scale size, K_o^{-1}. The index of refraction

variance $\langle n_1^2 \rangle$ can be calculated if $dn/d\rho$ is known and then Eq.(21) and (25) used to find $A_\psi = 1.5 \langle n_1^2 \rangle K_o^{-1} k^2 \Delta z$ from which $\alpha = 4.4 A_\psi (bk)^{-5/6}$ can be determined. The ratio of the anti-Stokes power in the presence of turbulence to that without is then $\tilde{I}_3/I_3 = (1 + \alpha L^{5/3})^{-1}$ with L being the distance from the beam waists to the turbulent layer. This simple calculation should indicate whether or not a CARS experiment is feasible in a given situation.

It is also worth reiterating that if the beam diameters as they penetrate the turbulent layer are smaller than the smallest scale phase perturbations then the beams are simply deflected without loss of instantaneous power density or coherence. In the coaxial beam case the CARS process is completely unaffected except for a small fluctuation in the direction of the emerging anti-Stokes radiation. If, however, a crossed beam geometry is used the pump and Stokes beams are deflected independently with the result that the average overlap of the beams is reduced and the signal degraded.

REFERENCES

1. A. C. Eckbreth and R. J. Hall, "CARS Thermometry in a Sooting Flame," Combust. Flame 36, 87-98 (1979).

2. R. L. Farrow, P. L. Mattern and L. A. Rahn, "Comparison Between CARS and Corrected Thermocouple Temperature Measurements in a Diffusion Flame," Appl. Opt. 21, 3119-3125 (1982).

3. I. A. Stenhouse, D. R. Williams, J. B. Cole and M. D. Swords, "CARS Measurements in an Internal Combustion Engine," Appl. Opt. 18, 3819-3825 (1979).

4. D. V. Murphy, M. B. Long, R. K. Chang and A. C. Eckbreth, "Spatially Resolved Coherent Anti-Stokes Raman Spectroscopy from a Line Across a CH_4 Jet," Opt. Lett. 4, 167-169 (1979).

5. E. K. Gustafson, J. C. McDaniel and R. L. Byer, "High Resolution Continuous-Wave Coherent Anti-Stokes Raman Spectroscopy in a Supersonic Jet," Opt. Lett. 7, 434-436 (1982).

6. See for example the review by H. C. Anderson and B. S. Hudson, Molecular Spectroscopy, Vol. 5, R. F. Barrow et al., ed., The Chemical Society, London (1978), pp. 142-201.

7. A. C. Eckbreth, "BOXCARS: Crossed-Beam Phase-Matched CARS Generation in Gases," Appl. Phys. Lett. 32, 421-423 (1978).

8. G. C. Bjorklund, "Effects of Focusing on Third Order Nonlinear Processes in Isotropic Media," IEEE J. Quantum Electron. 11, 287-296 (1975).

9. S. Guha and J. Falk, "The Effects of Focusing on the Efficiency of Coherent Anti-Stokes Raman Scattering," J. Chem. Phys. 75, 2599-2602 (1981).

10. R. F. Lutomirski and H. T. Yura, "Propagation of a Finite Optical Beam in an Inhomogeneous Medium," Appl. Opt. 10, 1652-1658 (1971).

11. H. T. Yura, "Mutual Coherence Function of a Finite Cross Section Optical Beam Propagating in a Turbulent Medium," Appl. Opt. 11, 1399-1406 (1972).

12. D. A. Kleinman, "Theory of Second Harmonic Generation of Light," Phys. Rev. 128, 1761-1775 (1962).

13. W. M. Shaub, A. B. Harvey and G. C. Bjorklund, "Power Generation in Coherent Anti-Stokes Raman Spectroscopy with Focused Laser Beams," J. Chem. Phys. 67, 2547-2550 (1977).

14. J. W. Goodman, Introduction to Fourier Optics, McGraw-Hill, New York (1968), p. 45.

15. V. I. Tatarskii, Wave Propagation in a Turbulent Medium, McGraw-Hill, New York (1961), pp. 124-128.

16. I. S. Gradshteyn and I. M. Ryzhik, Tables of Integrals, Series and Products, Academic Press, New York (1965), p. 319, Formula 3.383.8 and p. 1059 Formulae 9.220.1-4.

17. Reference 16, p. 686, Formula 6.565.4

18. M. Abramowitz and I. A. Stegun, Handbook of Mathematical Functions, National Bureau of Standards, Washington (1964), p. 375, Formulae 9.6.2 and 9.6.10.

19. S. M. Wandzura, "Meaning of quadratic structure functions," J. Opt. Soc. Am. 70, 745-747 (1980).

20. Reference 18, p. 362, Formula 9.1.21.

21. Reference 16, p. 716, Formulae 6.631.1 and 6.631.4.

22. Reference 18, p. 505, Formula 13.1.27.

23. F. K. Owen, C. C. Horstman, and M. I. Kussoy, "Mean and Fluctuating Flow Measurements of a Fully Developed Non-adiabatic Hypersonic Boundary Layer," J. Fluid Mechanics 70, 393 (1975).

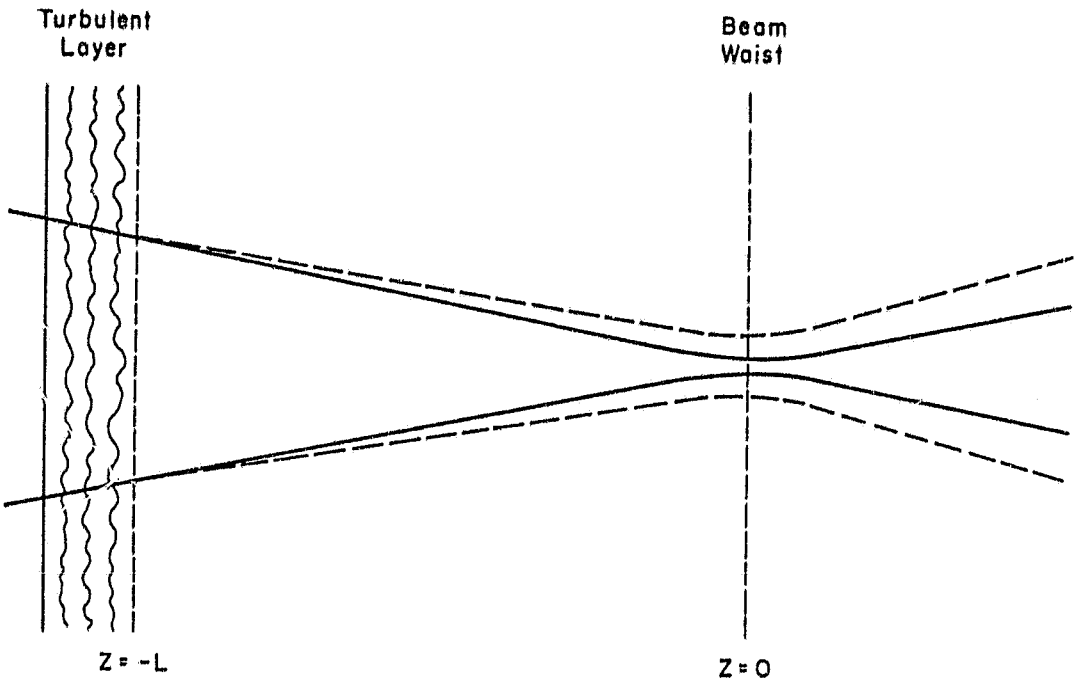

Figure 1. Illustration of the increase in the mean diameter of a beam wave due to a turbulent layer.

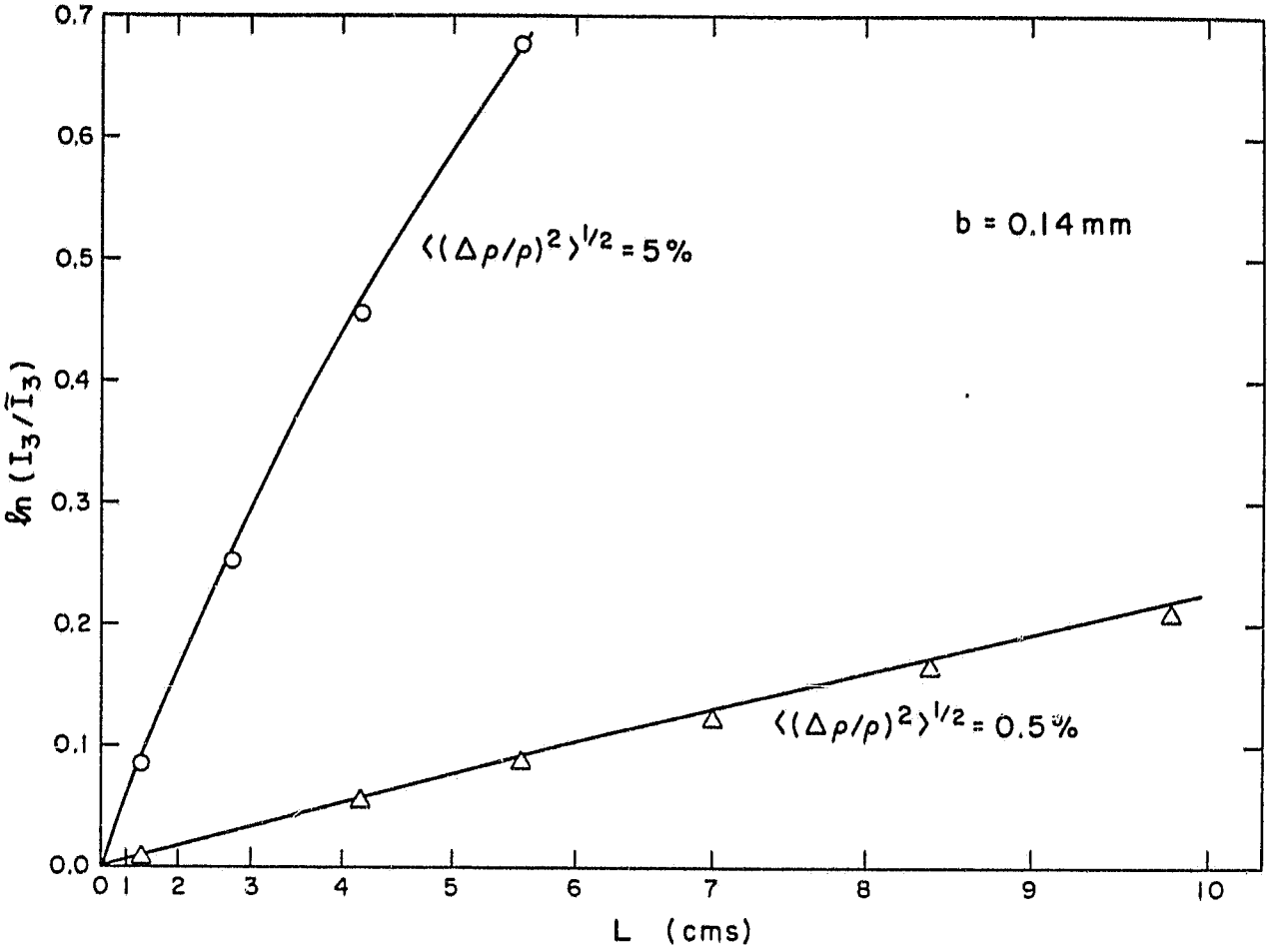

Figure 2. Logarithm of the ratio of the unperturbed anti-Stokes power to that perturbed by a phase screen versus $L^{5/3}$. Δ, O - values calculated by numerical integration of Eq.(36). Solid lines: $\ell n(1 + 2L^{5/3})$ with $\alpha = 5.5 \times 10^{-3}$ and 5.5×10^{-2} $cm^{-5/3}$ corresponding to rms density fluctuations of 0.5 and 5% respectively. Confocal parameter b = 0.14 mm, i.e., 1 cm diameter beam focused by a 10 cm fl lens.

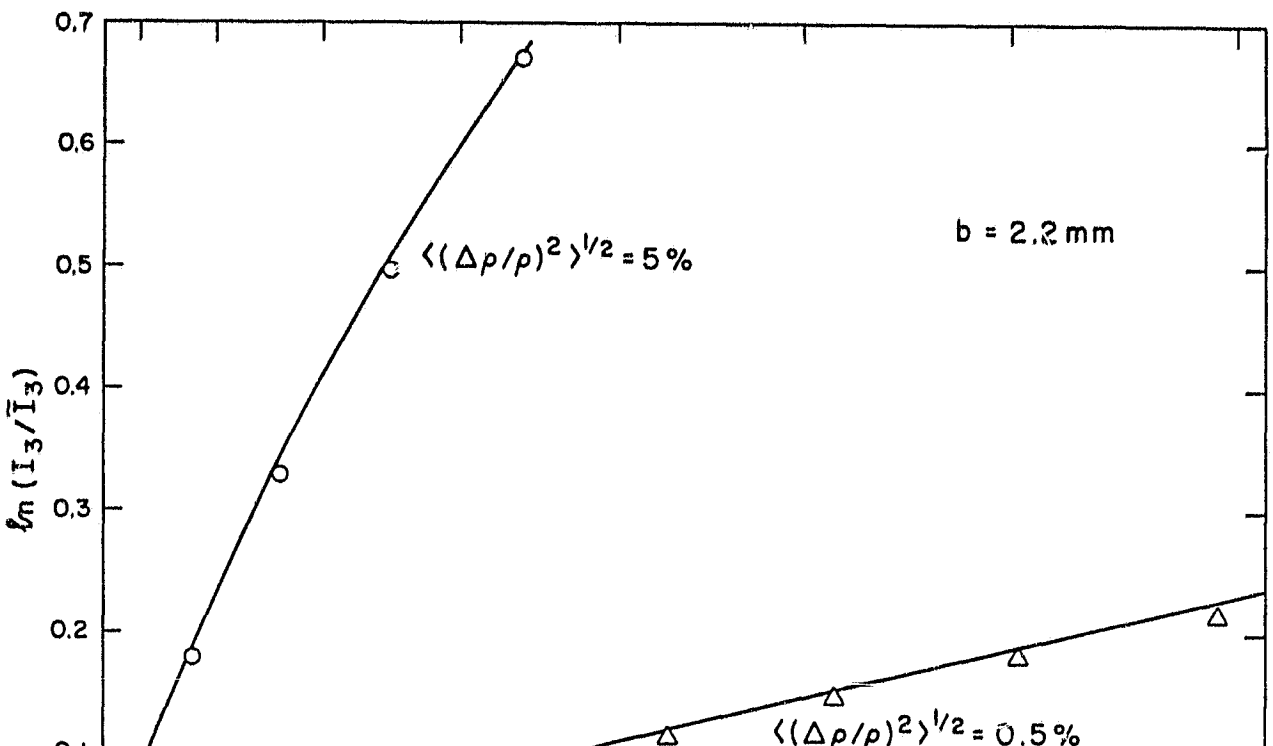

Figure 3. Same as figure 2 except b = 2.2 mm corresponding to a 1 cm diameter beam focused with a 40 cm fl lens. In this case $\alpha = 5.5 \times 10^{-4}$ and 5.5×10^{-3} for $\langle(\Delta\rho/\rho)^2\rangle^{1/2} = 0.5$ and 5% respectively.